

Matthias Tomczak · Lindsay Pender · Sharon Liefbrink

Variability of the Subtropical Front in the Indian Ocean south of Australia

Received: 15 August 2003 / Accepted: 19 February 2004
© Springer-Verlag 2004

Abstract A detailed high resolution survey of a small region (68×68 km) of the Subtropical Front south of Australia over a period of 14 days is used to study the interaction between the mixed layer and the permanent frontal structure underneath during summer conditions. The front extends through the mixed layer as a salinity front, while its temperature structure is modified by seasonal warming. Wind-driven movement of the mixed layer combines with the short-time development of indentations and filaments in the front to produce some degree of decoupling between the mixed layer and the underlying structure, and the front is not always found at the same location in and below the mixed layer. Intrusions and parcels of distinct water properties are found just below the mixed layer, produced as a result of the relative movement of the front in and below the mixed layer. These parcels are typically 10 km in width and 10–50 m in depth. Successive surveys of the front with a time separation of 2 days showed that these features persist over at least 1 week. Large scale surveys of the front show that parcels are ubiquitous along the Subtropical Front over a distance of several hundred kilometres. The results suggest that any study aimed at understanding the intricate interaction between the mixed layer and the layers below in oceanic fronts will have to address wind-driven dynamics and frontal dynamics together.

Keywords Front · Mixing · South Indian Ocean

Responsible Editor: Neville Smith

M. Tomczak (✉) · S. Liefbrink
Flinders University, School of Chemistry,
Physics and Earth Sciences,
6PO Box 2100, Adelaide SA 5048, Australia
e-mail: matthias.tomczak@flinders.edu.au

L. Pender
CSIRO Marine Research, 6PO Box 1538,
Hobart Tas 7001, Australia

Introduction

The region between the core of the trade winds and the maximum westerlies, which stretches around the globe between approximately 20° and 45° on either side of the Equator, is characterised by negative wind-stress curl in the atmosphere and by associated Ekman transport convergence in the ocean. In oceanography, this region has therefore become known as the Subtropical Convergence. Its hydrography shows a decrease in sea-surface temperature (SST) from the tropics to the temperate zones, accompanied by a decrease in sea-surface salinity (SSS). As a general rule, the poleward increase of surface density produced by the decrease in SST is larger than the decrease of surface density produced by the decrease in SSS, and as a consequence surface density increases with distance from the Equator.

Embedded in the Subtropical Convergence and somewhat on its poleward side is a zonal band of enhanced meridional SST and SSS gradients known as the Subtropical Front (STF). In the Southern Hemisphere this front can be described as beginning off the coast of Argentina as the southern boundary of the Brazil Current, stretching across the Atlantic Ocean at about 40° S, then passing south of Africa and continuing along that latitude through the Indian and central Pacific Oceans, where it eventually shifts northward to arrive at the coast of Chile as far north as 30° S (Tomczak and Godfrey 2003). It defines the southern limit of the subtropical gyres and separates them from the broad westward flow of the Circumpolar Current further south (Stramma and Peterson 1990; Stramma 1992; Stramma et al. 1995). In some regions the STF can divide into multiple fronts which can be quasipermanent features (Belkin and Gordon 1996).

Compared with other frontal systems of the world ocean, the Subtropical Front is relatively weak, displaying a temperature contrast of about 2° C and a salinity contrast of about 0.5 over a distance of 200 km. This combines with large short-term and seasonal variability of its location and a high incidence of eddy for-

mation and eddy shedding and explains why the STF is rarely seen in atlas data of ocean climate properties based on long-term mean distributions. The STF is, however, a very distinct feature in any meridional crossing of the subtropics and can be seen in synoptic data to at least 250 m depth.

A particular characteristic of the STF south of Australia is the degree of density compensation across the front. Stramma (1992) shows that east of South Africa the STF is associated with a geostrophic transport of some 30 Sv ($1 \text{ Sv} = 10^6 \text{ m}^3 \text{ s}^{-1}$) and that this transport is reduced to 10 Sv as Australia is approached. South of Australia it decreases further, reaching negligible magnitude east of 130°E (Schodlok et al. 1997; Schodlok and Tomczak 1997). This indicates that the effects of the temperature and salinity changes across the STF on density compensate for each other more and more from west to east.

The location of the STF on the poleward side of the Subtropical Convergence places it on the southern edge of the atmospheric high-pressure belt of the subtropics. This is the region where atmospheric frontal systems travel eastward, exposing the oceanic surface layer to strong winds with systematic changes in wind direction. As a result, currents in the upper ocean vary on the

atmospheric synoptic time scale, moving the water back and forth and shearing the upper mixed layer off from the underlying oceanic structure. Inertial oscillations, which are vertically uncorrelated, contribute to the differential horizontal movement of the water column. On longer time scales there is also a baroclinic response due to atmospherically forced sea-level variability.

The effect of this shearing movement depends on the direction of the movement itself. If the mixed layer is displaced poleward, water of low density is moved over denser water. This enhances the stability of the water column and produces a strong thermocline at the bottom of the mixed layer. The process can be reversed by moving the surface layer back to its original position. If, on the other hand, the mixed layer is displaced equatorward, the surface layer is pushed into a region where the underlying water is less dense. This produces convection and makes the process irreversible: if the surface layer is returned to its original position, its SST and SSS properties have changed, and a volume of mixed water remains below the mixed layer at the location where the convection occurred during the period of equatorward displacement of the surface layer.

This paper describes an experiment performed to document the effect of mixed layer movement on the structure of the Subtropical Front. It focuses in particular on the time history of the stratification during the passage of a strong wind system over the frontal region. The results indicate that the variability of the wind-driven flow in the presence of strong frontal salinity and temperature gradients is responsible for enhanced interleaving and patchiness at and below the seasonal thermocline not only in the front itself but over a wider region in its vicinity. As the seasonal thermocline is often associated with accumulation of plankton and particulate matter, the observed patchiness is likely to have important implications for marine life.

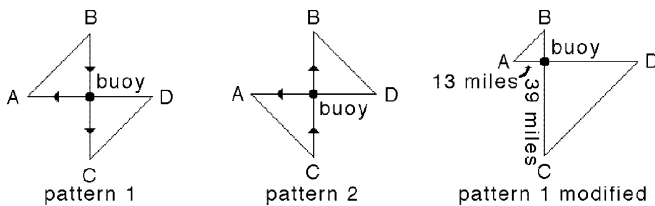
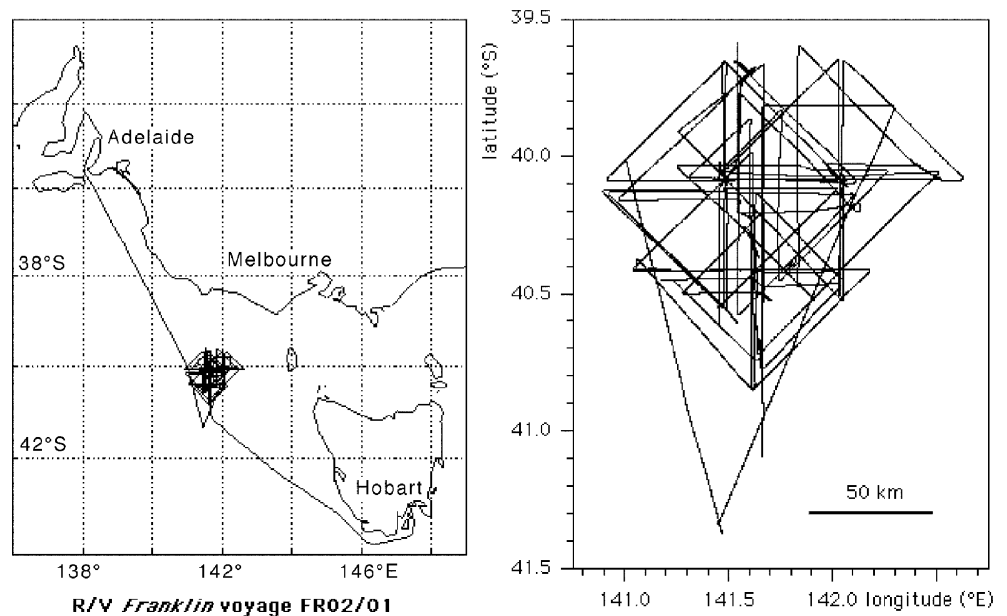


Fig. 1 The alternating patterns followed by the Seasoar tows, and the modified pattern used to readjust the study area with the frontal position. The modified pattern was used only once

Fig. 2 The cruise track of R/V Franklin voyage FR02/01



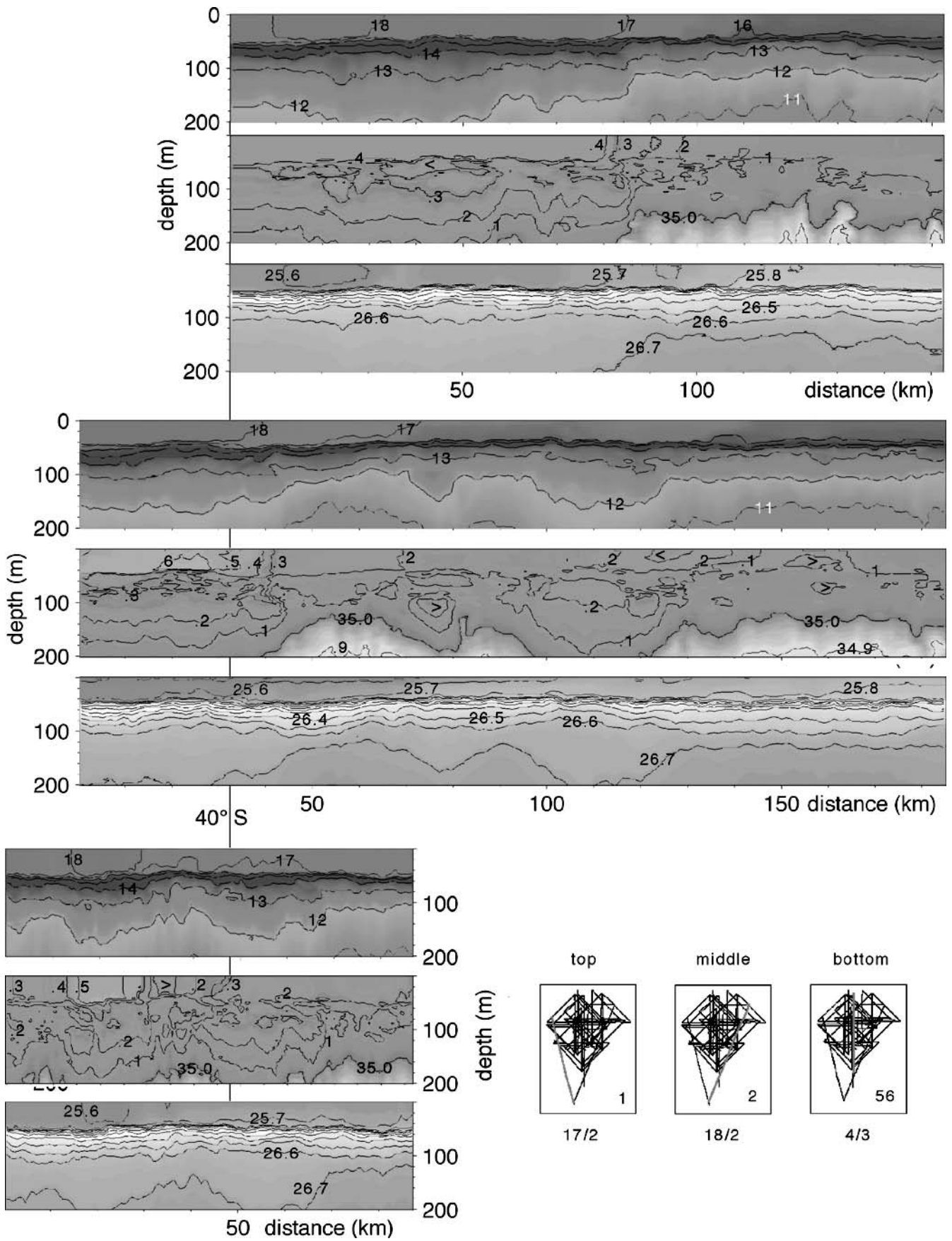


Fig. 3 Temperature ($^{\circ}\text{C}$), salinity and density (σ_t) along sections 1 (*top*) and 2 (*middle*) of 17–18 February and along section 56 (*bottom*) of 4 March. All sections are shown with north *to the left*

Data and methods

The data were collected during voyage FR02/01 of R/V *Franklin* between 16 February and 6 March, 2001. The study was designed to investigate mixing processes in an oceanic front on space scales of several kilometres and time scales typical of the passage of synoptic weather systems under conditions of partial or complete density compensation. The location of the study area was determined from knowledge of the regional position of the STF gained during two previous research voyages (James et al. 2002) and from satellite SST information available before the cruise.

A buoy drogued at 70 m depth was placed in the front and used as reference for a repeated survey pattern across the front. The survey covered a square of 36.8 nautical miles side length and followed two patterns (pattern 1 and pattern 2 in Fig. 1) in alternating fashion. Each pattern took about 1 day to complete. As a result, each of the two diagonals, 52 nautical miles in length, was repeated once every day, while the side transects were completed once every 2 days.

At one stage during the experiment it became apparent that the buoy had moved somewhat north from the STF. The survey was therefore adjusted to the modified pattern shown in Fig. 1. This modified pattern was followed for only 1 day.

The buoy initially followed the water movement at 70 m depth but lost its drogue at some time during the survey. This was only noticed when the buoy was recovered after the end of the experiment, and the exact moment when the loss of the drogue occurred is not known. Analysis of the Seasoar data indicates that it may have occurred on the 28th of February; this issue will be discussed further in a later section.

The instruments used for the survey were a Seasoar and an acoustic Doppler current profiler (ADCP). Continuous SST and SSS information was available from a thermosalinograph. The Seasoar is a remotely controlled device fitted with a dual CTD system which is towed behind the ship at a speed of 8 knots (1 knot = 1.852 km h^{-1}) and undulates over a depth range of up to 300 m. For the present investigation the flight path was set to cover the depth range 2–200 m, which gives it a time between successive dives of less than 4 min or a distance between dives of 1 km.

The Seasoar was recovered every 24–36 h and calibrated by placing the dual CTD system into a seawater bath. Additional calibration checks were made against CTD data. CTD stations were performed to 1500 m depth.

The raw Seasoar data were averaged to 1 m depth increments and converted into vertical CTD-type casts with 1 min time separation through interpolation. Casts

were geo-located using the ship's GPS positions, corrected by the distance between the ship and the Seasoar, which varied typically between 390 and 440 m depending on the instrument's dive depth. Data from CTD stations were likewise subsampled to 1 m depth increments.

The Seasoar data were generally of very high quality and required very little editing. Small data gaps (caused, for example, by temporary clogging of the conductivity cells) were filled by vertical interpolation. Data gaps exceeding 10 m in vertical extent were filled by horizontal interpolation between neighbouring casts.

In order to compare the frontal structure and evaluate its evolution between repeat sections, east-west sections were interpolated to constant longitude increments, north-south sections to constant latitude increments and all other sections to constant distance increments along the track. The interpolation increment was 0.01° latitude (approximately 1.11 km), 0.01° longitude (approximately 0.85 km) and 1 km in distance. Every second north-south section was inverted in direction to match the orientation of the other north-south sections.

The ADCP data were processed by the CSIRO Marine Research data centre support staff for R/V *Franklin*. The standard processing procedure produces current profiles relative to the ship based on 20-min averages and on 1-h averages with associated information (number of pings used for the average, number of good data received, bin length, depth of first bin, number of bins etc.). Ship speed and direction are averaged to match the ADCP data and also supplied as part of the standard processed data set.

During the research voyage reported here the bin size of the ADCP was set to 8 m, and the first usable bin was centred on 16.8 m depth. We removed spikes from the ADCP data and calculated absolute current velocities for both the 20-min and the 1-h average profiles from the ADCP and ship speed and direction data supplied by CSIRO.

Meteorological data were recorded every 10 s and processed into time series of 5 min resolution. They include air pressure, 5 min average wind speed, 5 min average wind direction and maximum wind speed (wind gust) for the 5 min period.

Results

Figure 2 shows the study area and the accumulated cruise track for the voyage. On arrival at the likely study area, R/V *Franklin* performed two long Seasoar tows to survey the hydrographic situation. Figure 3 shows the temperature, salinity and density distribution along the two tows.

The STF is commonly identified by the location where the 12°C isotherm crosses the 150 m (Nagata et al. 1988) or 200 m (Orsi et al. 1993) depth level. During winter the 12°C isotherm reaches the sea surface, usually not far from where it rises through the 150–200-m depth level. The STF is then also easily identified in surface temperature observations.

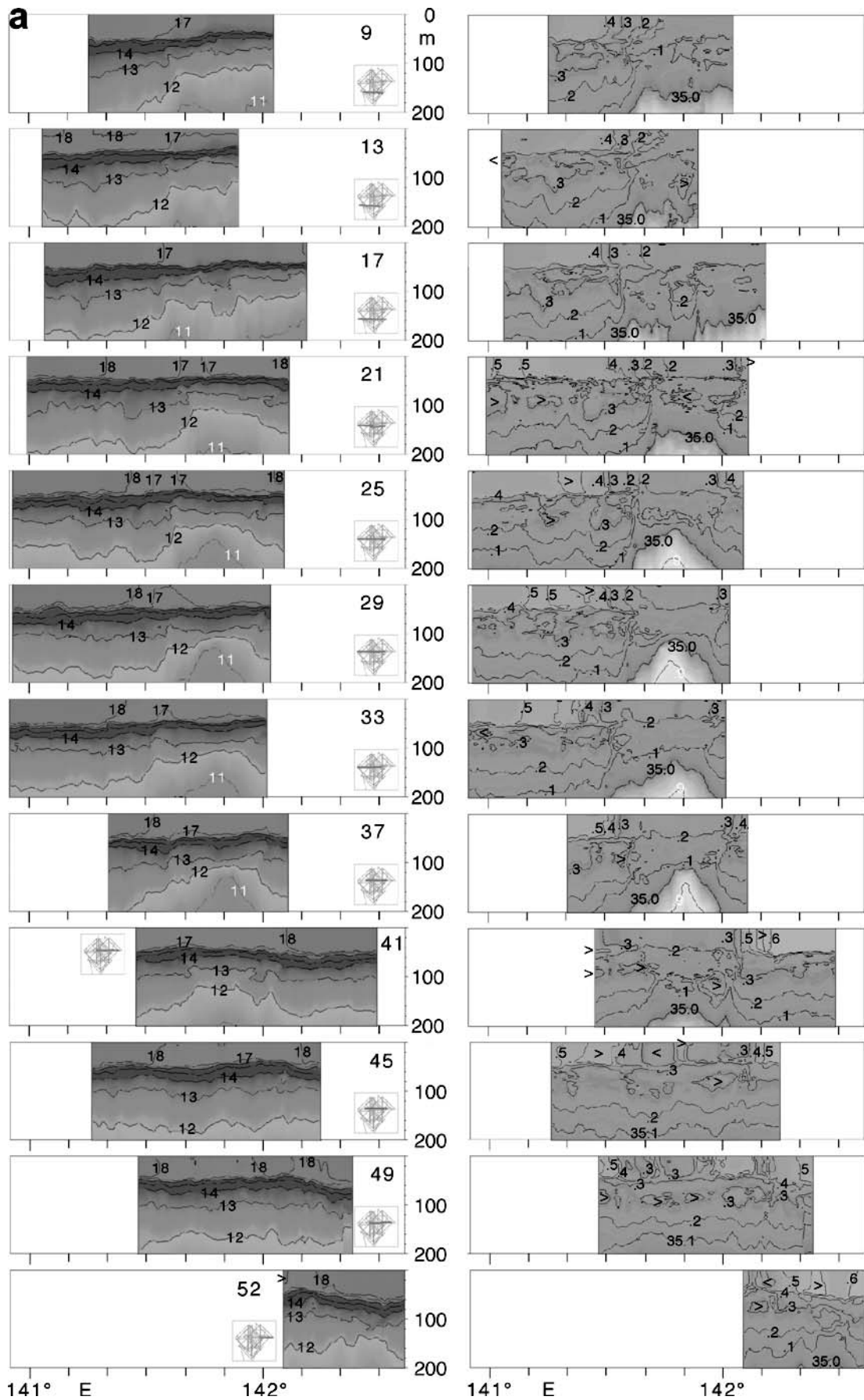


Fig. 4 Temperature ($^{\circ}\text{C}$), salinity, current speed (ms^{-1}) and current direction ($^{\circ}$) along east-west sections, plotted against longitude. Section numbers are given in the *top right* of the temperature sections. Current speed is contoured every 0.1 m s^{-1} , current direction every 90° . The time interval between successive sections is approximately 2 days

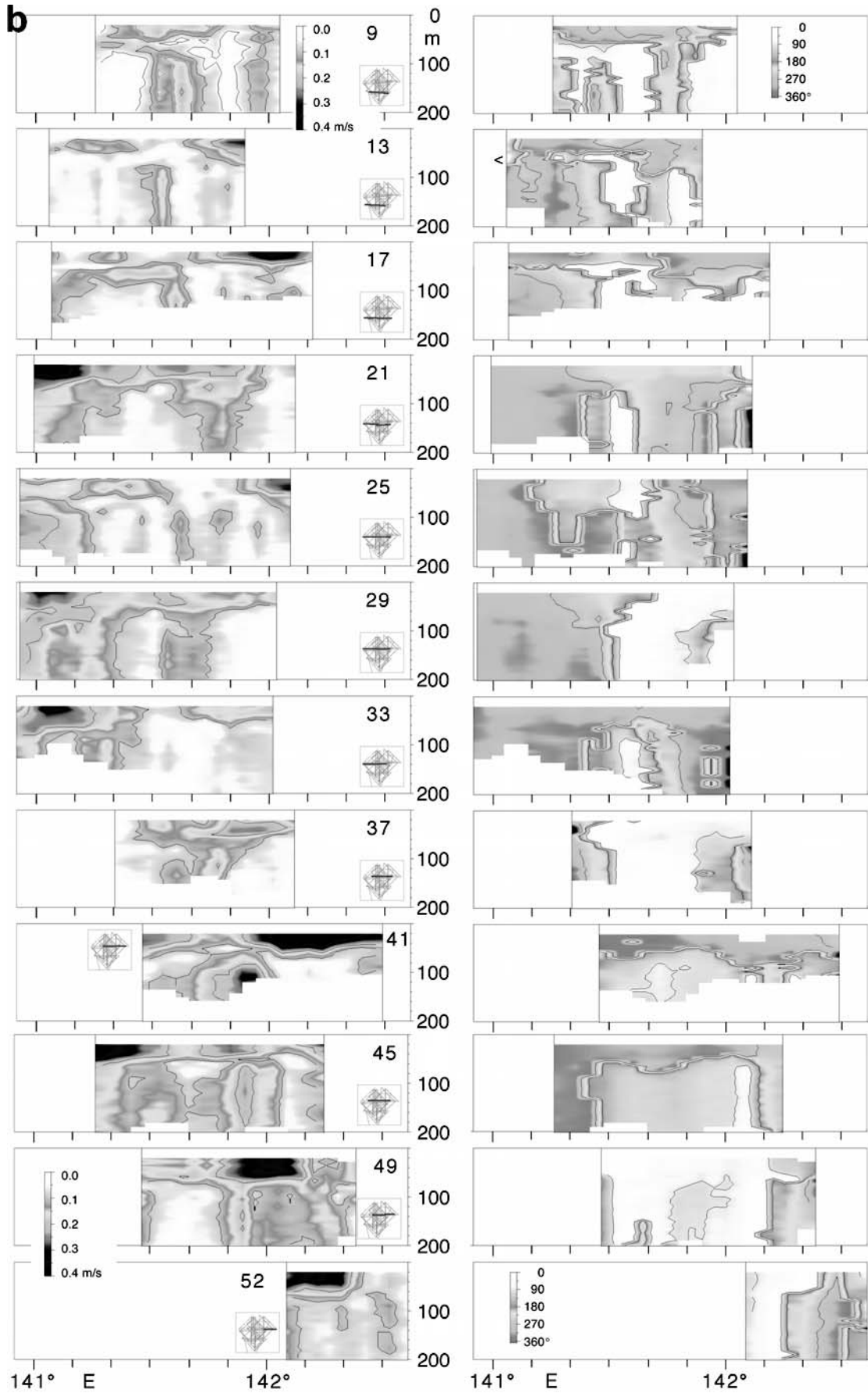


Fig. 4 (Contd.)

The presence of a warm surface mixed layer during summer makes the situation more complex. The STF is still identifiable through the position of the 12 °C isotherm relative to 150–200 m depth. At the surface it is also associated with a temperature front, but the enhanced horizontal temperature gradient is found at higher temperatures (14–18 °C depending on location).

James et al. (2002) point out that salinity is a more stable indicator of the frontal position since it does not undergo the same daily and seasonal variations as temperature. They identify the salinity range 34.9–35.4 as indicative of the STF.

In section 1 the 35.2 isohaline rises from about 150 m depth to the bottom of the mixed layer at km 85 (latitude 40°45'S; here and in the following kilometre references refer to the distance scale on the figures), where the 12 °C isotherm crosses the 150-m depth level and the 17 °C isotherm comes to the surface. The 35.2 isohaline then breaks the surface some 10 km further south at km 95 (latitude 40°51'S). A rise of the 26.7 isopycnal from 200 m to 140 m between km 85 and km 90 provides additional indication that the STF was located just south of latitude 40°45'S. The front is also clearly associated with a poleward decrease of the mixed-layer temperature from >18 to <17 °C.

The situation in section 2 is less obvious. The 150-m depth level crossing of the 12 °C isotherm, the 35.1 isohaline and the 26.7 isopycnal all indicate up to five crossings of the front (near kms 42, 72, 82, 105 and 120). This suggests a frontal orientation roughly parallel to the section and some degree of meandering. A clear change from cold, fresh subpolar conditions to the warm, saline environment of the subtropical side of the front occurs at km 40 (latitude 40°08'S), where the surface salinity changes from <35.3 to >35.4 and the 34.2 isohaline rises to the bottom of the mixed layer. In this section the distance between the surfacing of the 35.2 isohaline and its separation from the mixed layer is about 30 km. A significant change in the mixed-layer temperature is again associated with the STF.

Section 56, the final section of the experiment, is located about halfway between sections 1 and 2 but was taken 14 days later. Significant changes occurred during that period. A general southward decrease of the salinity in the mixed layer can still be seen; but no isohaline penetrates the mixed layer in a well-defined manner from depths of 150 m or more. The 35.2 isohaline is found at the bottom of the mixed layer both in the south (latitude 40°58.4'S) and in the north (latitude 39°41.6'S) of the section. It rises from about 130 m depth at various locations, but continuity through the mixed layer is not evident, even if significant movement of the mixed layer relative to the underlying structure is considered.

Figure 4 shows the development of the frontal structure in time as seen in the zonal sections, which were repeated daily. All sections were traversed from east to west. Sections 9–41 display strong similarity in their hydrographical structure. There is much less continuity of hydrographical features from section 41 to the

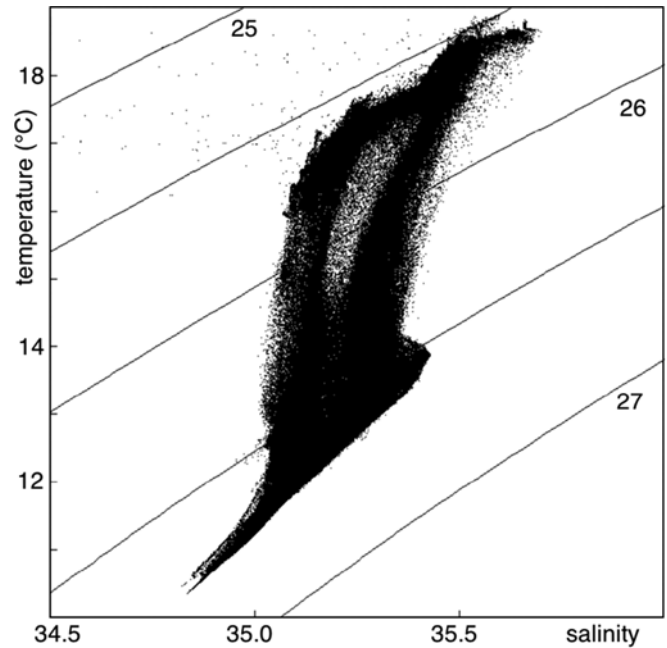


Fig. 5 Cumulative TS diagram of sections 1–56. Isopycnals are labelled in σ_t units

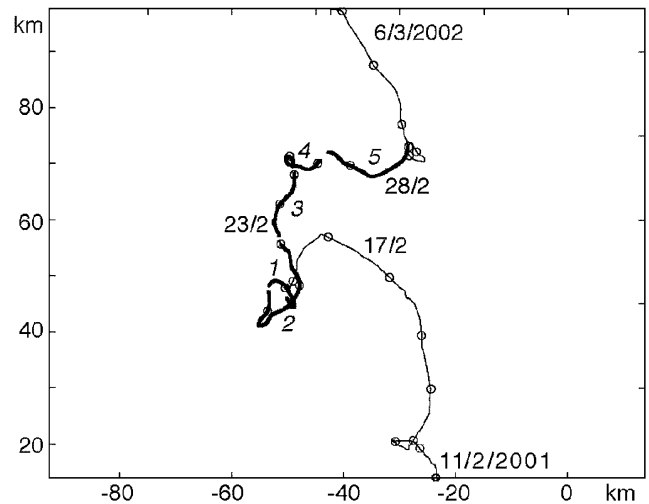


Fig. 6 Progressive vector diagram of wind, reduced to surface water movement (see text for details), from 11 February to 6 March based on the wind measurements on board R/V *Franklin*. Numbers next to heavy portions of the line indicate the periods of the five surveys of Fig. 10–12

following sections. This indicates that the buoy probably lost its drogue between sections 41 and 45, or possibly already shortly before section 41, and that the Seasoar sections obtained after section 37 no longer sampled the water body at the same location.

It has, of course, to be realized that the buoy was drogued at 70 m and that the water body above and below that depth can exhibit different movement. Independent movement of the mixed layer and the water below the mixed layer can be inferred from the change of the location where the 18 °C isotherm breaks the surface

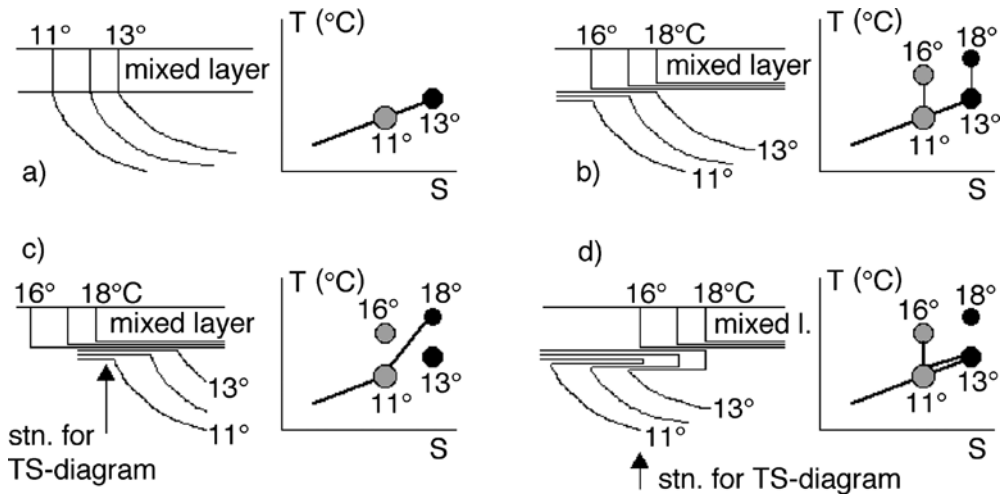


Fig. 7a–d Sketch of TS-diagrams in the STF. **a** Winter. The temperature front reaches through the mixed layer to the surface. The grey TS point gives TS properties on the cold side of the front, the black TS point represents the warm side. **b** Summer. Warming of the surface mixed layer raises the temperature on either side of the front by the same amount. The result is a surface temperature front at a higher temperature above the subsurface expression of the STF, which remains unchanged. **c** The STF during summer when the mixed layer is shifted poleward. Only water from the cold side of the front is found in the frontal region below the mixed layer; it is capped by water from the warm side of the mixed layer. The TS diagram reflects this transition from cold to warm. **d** The STF during summer when the mixed layer is shifted equatorward. Water from the warm side of the front is found below the mixed layer in the frontal region; it is capped by water from the cold side of the mixed layer. The TS diagram shows a strong salinity and temperature inversion

relative to the location where the 12 °C isotherm crosses the 150-m depth level. (As the sections were repeated every 24 h the effect of the daily temperature cycle is eliminated from the comparison.)

The position of the sections is shown relative to longitude, so the change in section position gives an indication of zonal movement of the marker buoy. Meridional movement can be estimated from the location of each section in the grid of all sections, indicated by the thick red line of the inset figures. It is seen that from section 17 to section 33 there was general weak westward movement. The strong eastward movement from section 37 onwards is most likely another indicator for the loss of the drogoue on the buoy. Northward movement occurred between sections 9 and 29, with not much meridional movement afterward.

The current information of Fig. 4 is based on the 20 min averages of the ADCP observations, which gives spatial information at about one fifth of the resolution of the Seasoar CTD data. At the beginning of the experiment (section 9) the ADCP data show relatively strong westward current in the mixed layer and distinct current shear between the mixed layer and the water below. The STF is associated with a jet-like current setting towards 0°–90°, which is flanked by sluggish flow in the opposite direction. Sections 13 and 17 show a similar situation, with some variation in the strength of the mixed-layer current. The currents in these sections

show that the salinity inversions just below the mixed layer are related to the front itself: the frontal jet extends into the intrusions in both speed and direction.

The situation becomes progressively confusing as time goes on, but in most sections the depth of the mixed layer remains associated with a sudden drop in current speed. Section 29 displays another frontal jet. The jet seen in section 45, on the other hand, appears not to be associated with a frontal structure or a significant change in direction.

Figure 5 displays the cumulative temperature–salinity (TS) diagram constructed from all Seasoar data of sections 1–56. The envelope of all data shows a nearly linear TS relationship at the lower temperature end connecting approximately the TS points (10.5 °C, 34.8) and (13.8 °C, 35.4) and representing Indian Central

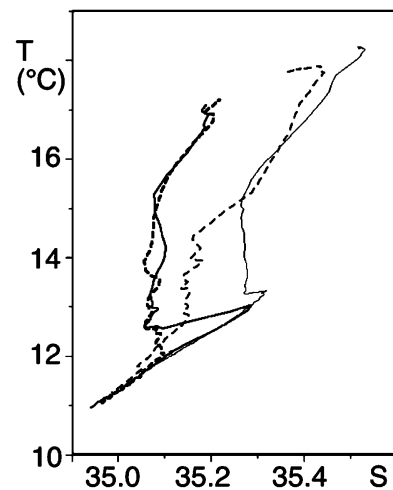
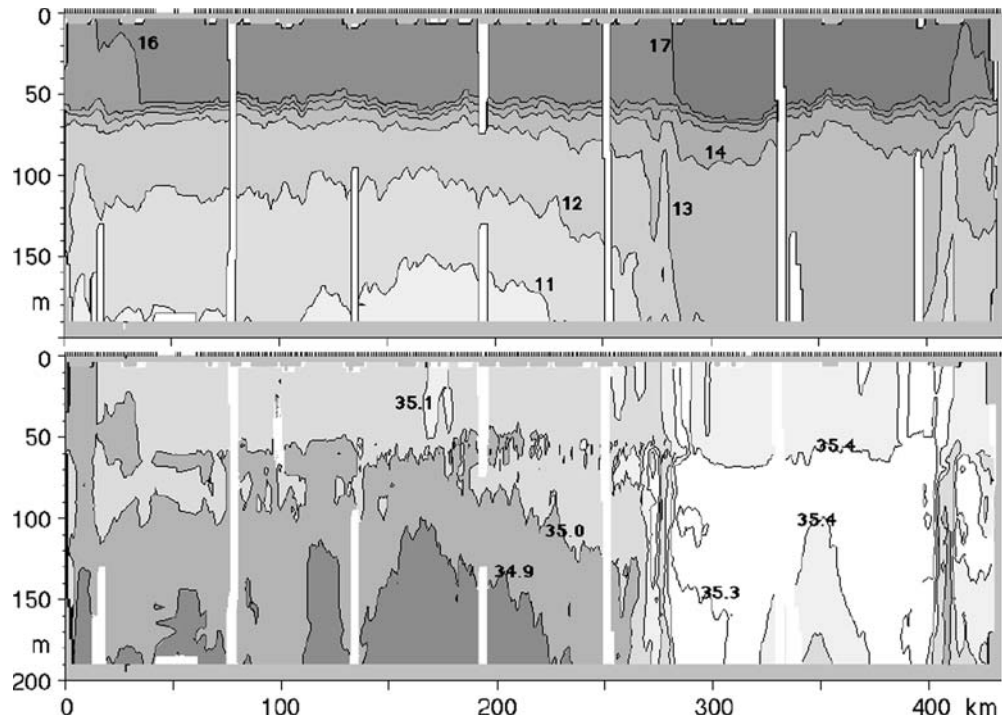


Fig. 8 Examples of TS diagrams to demonstrate the situations shown in the sketch of Fig. 7. All stations are taken from section 55, the last section to run from SE to NW across the study area. The thin line represents the situation on the subtropical side of the front, the heavy broken line the situation on the subpolar side. Both together correspond to the situation of Fig. 7b. The lighter broken line represents the situation shown in Fig. 7c, the full heavy line the situation shown in Fig. 7d. The kink towards lower salinity at the top of the lighter broken line indicates recent rainfall

Fig. 9 Temperature (°C, *top*) and salinity (*bottom*) along a transect made during February 1998 from approximately 39°45'S, 127° 53' E to 37° 23' S, 131° 30' E (summer transect T5 of James et al. 2003)



water (ICW), the water of the permanent thermocline of the region (Tomczak and Godfrey 2003). Points above this line represent the effect of seasonal warming (with little or no change in the evaporation/precipitation balance and therefore no significant change in the salinity) and are representative of the bottom of the mixed layer. The accumulation of points at the upper range of the envelope (close to the $\sigma_t = 25.6$ isopycnal) represents the mixed layer. Isolated scattered TS points at lower salinities indicate the effect of rainfall.

The presence of the front stands out clearly in the TS diagram. The connection between the ICW and the mixed layer occurs in two distinct clusters, representing the subtropical and the subpolar side of the front. TS points between the clusters are relatively scarce, particularly in the temperature range 14.5–17 °C. As the data were collected with a horizontal resolution of 1 km, this indicates that the width of the frontal zone is of the order of only a few km.

The TS line of Indian Central Water in Fig. 5 shows a double structure: at the low-temperature, low-salinity end two lines are seen to run parallel to each other. Similar parallel TS relationships have been observed in the vicinity of the STF south of Australia on earlier occasions, and the effect is definitely not a calibration problem. In the permanent thermocline of the subtropics ICW does not display multiple TS relationships but is characterized by a well defined unique TS line; but the STF is located in or very close to the formation region of ICW, where water in the thermocline has been subducted only recently. Multiple TS lines in the thermocline could therefore indicate variations in the atmospheric conditions during the active subduction period of successive years.

In order to estimate the effect of the local wind on water movement, surface water movement v_0 was calculated from wind speed w as

$$v_0 = \frac{0.0127w}{\sqrt{\sin \varphi}}$$

(Pond and Pickard 1991), where φ is the latitude (set to 40°S in this application). Figure 6 shows the resulting progressive vector diagram. Winds were mostly from the south but turned to northerly during 18 February for a few days; during 4 and 5 March the wind was predominantly westerly. The conversion to water movement applies to the sea-surface velocity and thus will overestimate the observed movement of the mixed layer derived from the buoy movement. Note also that no rotation has been applied; actual mixed layer movement can be expected to be to the left of the movement indicated in the figure to various degrees.

Discussion

It is useful to begin the discussion of STF dynamics with a schematic sketch of its hydrographical structure (Figure 7). In winter a meridional sequence of vertical TS diagrams across the front shows the well-known TS relationship of Indian Central Water, and the two sides of the front are associated with two TS points at the upper end of the TS relationship (Fig. 7a). During summer the STF is capped by a warm mixed layer but the salinity structure is barely changed. This raises the TS points from their winter position to a location at higher temperatures but nearly identical salinities (Fig. 7b). The front still has a surface expression in the

in the situation shown in Fig. 7d. Both situations and various variants of them can be seen in the data (Figure 8). The situation shown in Fig. 7d was seen quite frequently, while the situation shown in Fig. 7c was observed relatively rarely.

The vertical stability of the water column in Fig. 7c and d is fundamentally different. Moving the mixed layer poleward increases vertical stability, moving it equatorward can lead to instability and produce convection events that reach below the mixed layer. Double diffusion will also act to stir the water column. Data collected in the STF south of Australia on earlier occasions show many remnants of convection events below the mixed layer and/or double diffusive events.

Figure 9 is a temperature and salinity section obtained during a summer survey of the STF during 1998 (James et al. 2002). The section is located some 700 km west of the area visited for the current experiment and, with a total length of over 400 km, nearly five times as long as the longest section in Fig. 4. It shows multiple isolated pockets of low and high salinity at the bottom of the mixed layer, particularly in the vicinity of km 200–300. Similar structures can be seen in the salinity distribution observed during this experiment (sections 21–33, Fig. 4).

Note that the pockets seen in Fig. 9 are located on the subpolar side of the front. The schematic of Fig. 7d would indicate that remnants from earlier convection events should be found mainly on the subtropical side. The pockets may thus indicate that processes other than convective adjustment (for example double diffusion) are acting in the frontal region. Convection on the subtropical side of the STF may have been responsible for the observed weakening of the thermocline at the bottom of the mixed layer.

In an attempt to obtain a better understanding of the relative movement of the mixed layer and the water below, we constructed salinity maps from groups of sections. These groups consist of all sections from one completion of the patterns 1 and 2 in Fig. 1 and thus provide data along the perimeter and the two diagonals of a square. Such a data distribution requires substantial interpolation. To minimize boundary extrapolation effects we rotated the square by 45°.

Figure 10 shows the salinity at 20 m, representative of the mixed layer, and at 180 m depth, selected to indicate the location of the STF below the mixed layer. The frontal direction is from southwest to northeast throughout the observation period, but significant changes occurred in the shape of the front on the scale of the experiment. The most significant change is probably the indentation in the front at the surface that develops in the southwest during surveys 3 and 4, which disappears in survey 5, where it is replaced by another indentation in the east. The fact that the surveys did not all cover the same area makes it difficult to assess the permanence of some of the features; but it is evident from the salinity distribution at 20 m depth that the mixed layer did not follow a slab-like movement.

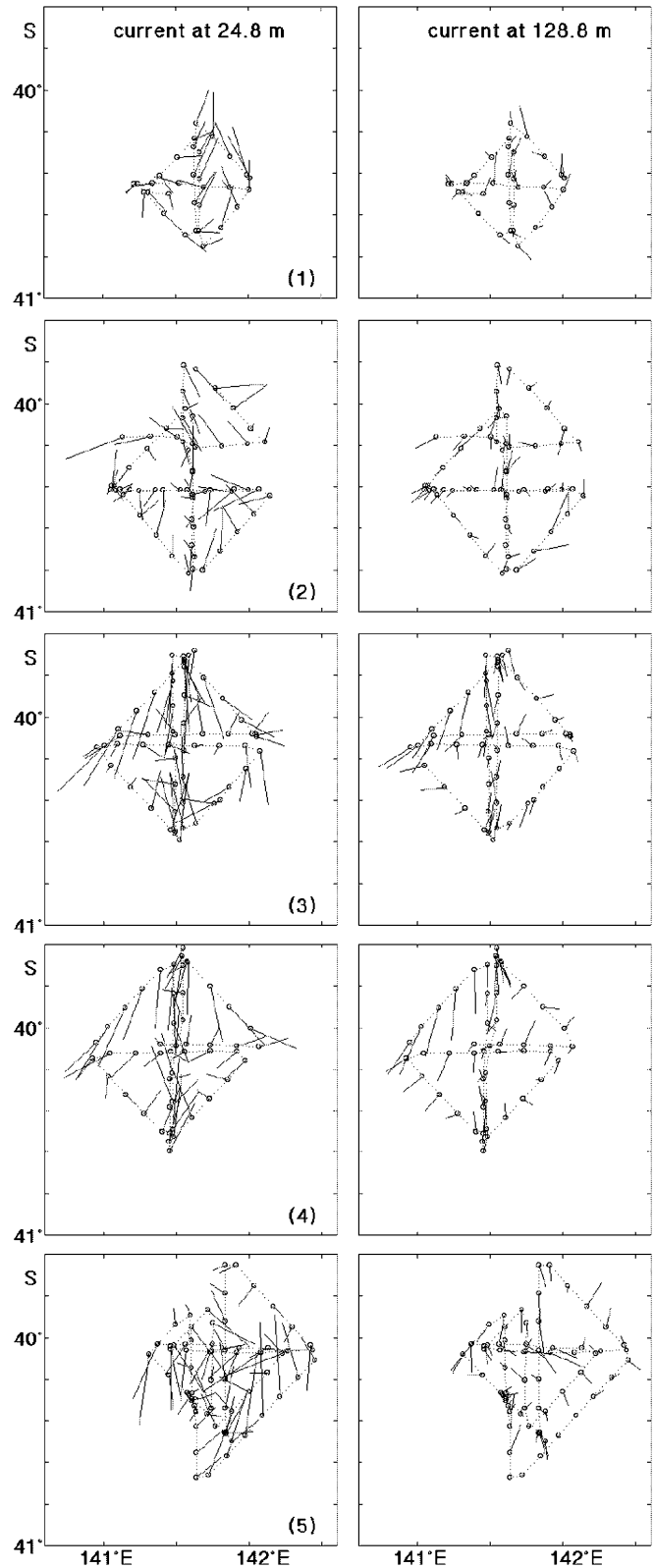


Fig. 11 Currents in the mixed layer (*left*) and below the mixed layer (*right*) based on 60 min ADCP averages. The surveys 1–5 are the same as in Fig. 10

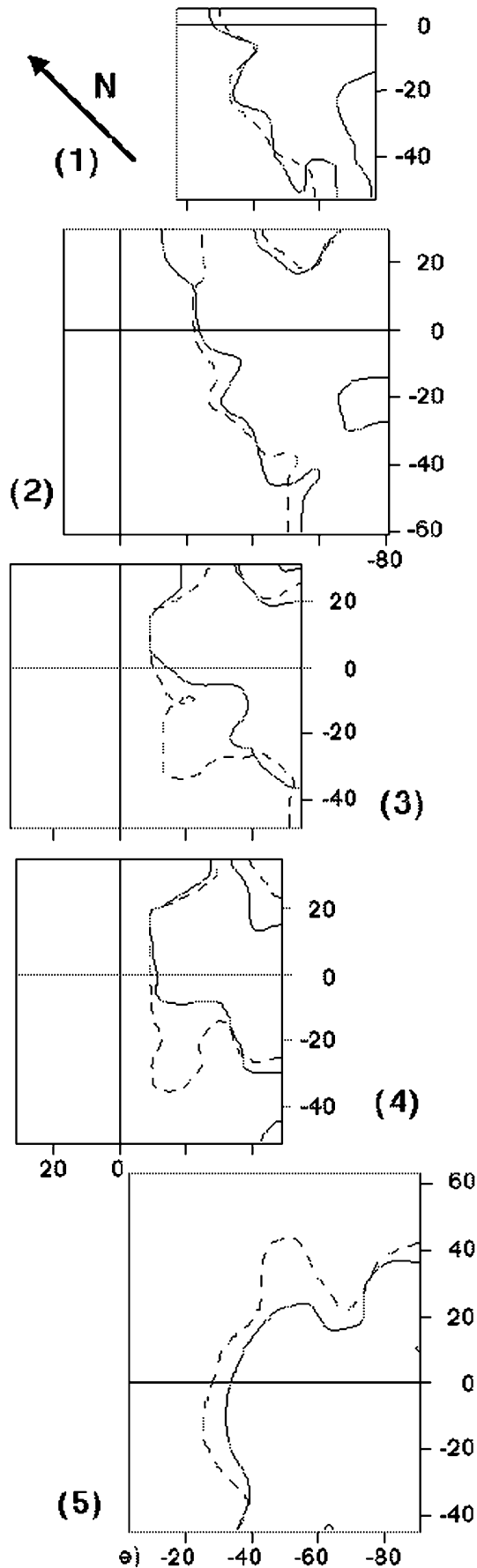


Fig. 12 Positions of the 35.35 isohaline in the mixed layer (at 20 m depth, broken line) and of the 35.10 isohaline below the mixed layer (at 152 m depth, full line). The surveys 1–5 are the same as in Fig. 10

The position of the front at the 180-m depth level reflects closely the frontal position found in the mixed layer. The isohalines show a similar degree of transient indentation. A centre of low salinity intensifies briefly during surveys 3 and 4 but is no longer seen in survey 5.

Figure 11 shows the currents, determined from 60-min averaged ADCP data, at depths comparable to Fig. 10. (24.8 and 128.8 m; data coverage was insufficient at bin depths closer to the 180 m level.) The observations include tidal currents; but each survey took 2 days to complete, and the fact that most surveys produce a reasonably smooth current field suggests that the current is not tidally dominated.

Survey 1 shows strong northward current on the subpolar (low-salinity) side of the front, particularly in the mixed layer. The current intensifies during survey 2 and swings towards northwest in the northern part of the survey area. This was the region covered during the second day of the survey, so the difference in current direction between the south and the north may actually indicate a development in time rather than space.

By the time of survey 3 the current turned around to southwestward. Current shear across the front is maintained, particularly below the mixed layer, where currents on the subpolar side of the front are now weak but still northward in places, while currents on the subtropical side follow the flow of the mixed layer. This situation is maintained and intensified during survey 4, which shows strong shear across the front also in the mixed layer. The apparent strong convergence in the flow field is again most likely an indication of time rather than space changes.

The most remarkable aspect of the final survey 5 is the large vertical current shear between the mixed layer and the underlying water.

The observed current distribution does not bear much relationship with Ekman layer movement as it would be expected from the observed winds (Fig. 6). It appears to be controlled by the dynamics of the front and associated eddies or other instabilities. A comparison between positions of selected isohalines in and below the mixed layer demonstrates this even more. Figure 12 compares the isohaline 35.35 in the mixed layer with the isohaline 35.10 at 152 m depth, chosen because their positions coincided at the beginning of the experiment. It is seen that the two isohalines maintain their close position relationship in survey 2 but separate in the west during survey 3. The indentation or filament-like structure in the mixed layer grows during survey 4 but has disappeared in survey 5, which indicates the possible growth of another filament in the northeast.

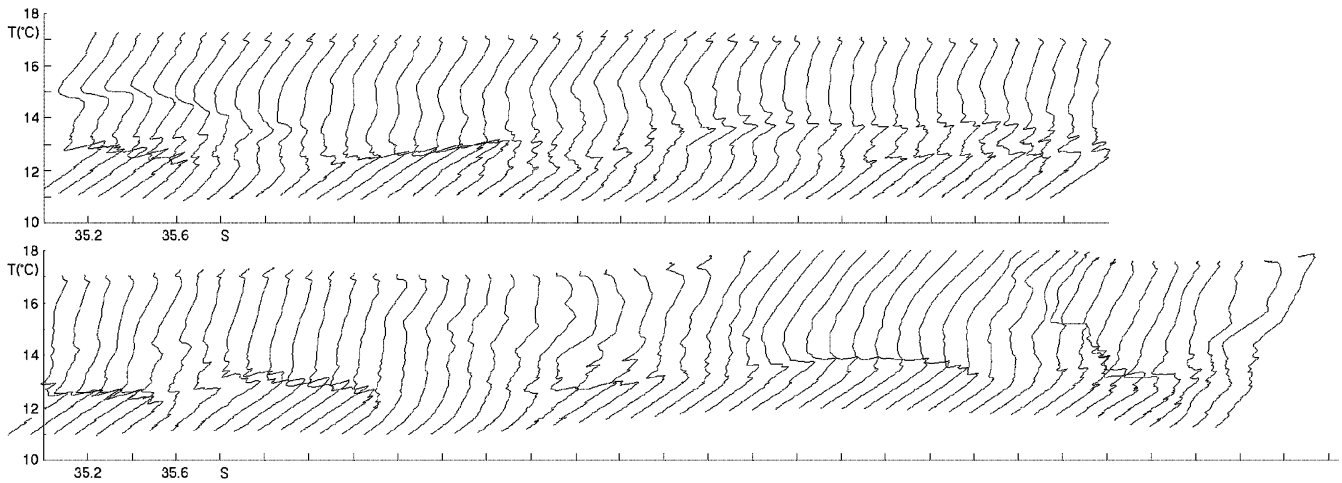


Fig. 13 TS diagrams for section 55. Successive diagrams are shifted in salinity by 0.1; the scale applies to the TS diagram of the first station. The sequence is *from left to right in the upper part* and continues *from left to right in the lower part*

Conclusion and summary

This experiment was performed to investigate the effects of the movement of the mixed layer, on time scales of synoptic weather variations, in a frontal region. When the experiment was planned it was anticipated that for space scales from a few kilometres to several tens of kilometres movement of the mixed layer could be described as slab movement driven by the wind.

It is certainly safe to assume that the wind field is reasonably uniform over that scale; the typical size of an atmospheric depression is an order of magnitude larger than the region studied here; but the results show that the assumption of slab movement is not tenable in the present situation, not even if it is applied to both sides of the front separately and allowance is made for strong current shear across the front. It is well known that the Subtropical Front is highly variable in strength and position, particularly in the Australian sector (Tomczak and Godfrey 2003), and the time evolution of the current field and associated movement of the various water layers appear to be determined more by frontal dynamics than by slab movement of the mixed layer.

Wind forcing is, of course, responsible for the observed differences in mixed-layer movement and movement at greater depth. Any study aimed at understanding the intricate interaction between the mixed layer and the layers below in oceanic fronts will thus have to address wind-driven dynamics and frontal dynamics together. This is not a trivial task, and it may be questioned whether it is possible at all with our present technology. Figure 13 shows a sequence of TS diagrams from the Seasoar casts of section 55 (the same section that supplied the example diagrams of Fig. 8). The effect of shifting the mixed layer back and forth over the underlying frontal structure is seen in the multiple

regions with strong salinity intrusions. Some groups of stations indicate the presence of intrusions at more than one depth, which would indicate that intrusions can persist over periods longer than the time it takes an atmospheric depression to pass through the region; the lower intrusions would have to be produced during a period of stronger wind and thus greater-mixed layer depth. The spacing between successive Seasoar profiles is about 1 km, so the typical extent of the intrusions is of the order of 10 km. A detailed study of the time history of these features would require a resolution of 10 km or better in three dimensions. Seasoar resolves that scale in two-dimensional cross-sections but is unable to document the three-dimensional evolution.

Despite these shortcomings, the dataset collected during the experiment can most likely provide more insight into the time history of intrusions. Pattern matching and neural networks are two techniques that could offer possible avenues for further analysis. These possibilities are currently being investigated.

References

- Belkin IM, Gordon AL (1996) Southern Ocean fronts from the Greenwich meridian to Tasmania. *J Geophys Res* 101: 3675–3696
- James C, Tomczak M, Helmond I, Pender L (2002) Summer and winter surveys of the Subtropical Front of the south eastern Indian Ocean 1997–1998. *J Mar Systems* 37: 129–149
- Nagata Y, Michida Y, Umimura Y (1988) Variation of positions and structures of the oceanic fronts in the Indian Ocean sector of the Southern Ocean in the period from 1965 to 1987. In: Sahrhage D (ed): *Antarctic ocean and resources variability*, Springer, Berlin Heidelberg New York, pp 92–98
- Orsi AH, Nowlin WD jr, Whitworth T III (1993) On the circulation and stratification of the Weddell Gyre. *Deep-Sea Res* 42: 169–203
- Pond S, Pickard GL (1991) *Introductory dynamical oceanography*, 3rd ed.. Butterworth Heinemann, Oxford, 329 pp
- Schodlok MP, Tomczak M (1997) The circulation south of Australia derived from an inverse model. *Geophys Res Lett* 24: 2781–2784
- Schodlok MP, Tomczak M, White N (1997) Deep sections through the South Australian Basin and across the Australian-Antarctic Discordance. *Geophys Res Lett* 24 :2785–2788

- Stramma L (1992) The South Indian Ocean Current. *J Phys Oceanogr* 22: 421–430
- Stramma L, Peterson RG (1990) The South Atlantic Current. *J Phys Oceanogr* 20: 846–859
- Stramma L, Peterson RG, Tomczak M (1995) The South Pacific Current. *J Phys Oceanogr* 25: 77–91
- Tomczak M, Godfrey JS (2003) *Regional oceanography: an introduction*. 2nd ed, Daya, Delhi, 390 pp